



**HAL**  
open science

# Dynamics of the viral community on the cheese surface during maturation and persistence across production years

Thomas Paillet, Quentin Lamy-Besnier, Clarisse Figueroa, Marie-Agnès Petit,  
Eric Dugat-Bony

## ► To cite this version:

Thomas Paillet, Quentin Lamy-Besnier, Clarisse Figueroa, Marie-Agnès Petit, Eric Dugat-Bony. Dynamics of the viral community on the cheese surface during maturation and persistence across production years. 2024. hal-04416953

**HAL Id: hal-04416953**

**<https://hal.inrae.fr/hal-04416953>**

Preprint submitted on 25 Jan 2024

**HAL** is a multi-disciplinary open access archive for the deposit and dissemination of scientific research documents, whether they are published or not. The documents may come from teaching and research institutions in France or abroad, or from public or private research centers.

L'archive ouverte pluridisciplinaire **HAL**, est destinée au dépôt et à la diffusion de documents scientifiques de niveau recherche, publiés ou non, émanant des établissements d'enseignement et de recherche français ou étrangers, des laboratoires publics ou privés.



Distributed under a Creative Commons Attribution - NonCommercial - NoDerivatives 4.0 International License

1 Dynamics of the viral community on the cheese surface during maturation and persistence  
2 across production years

3

4 Thomas Paillet,<sup>a</sup> Quentin Lamy-Besnier,<sup>b</sup> Clarisse Figueroa,<sup>a\*</sup> Marie-Agnès Petit,<sup>b</sup> Eric  
5 Dugat-Bony<sup>a#</sup>

6 <sup>a</sup>Université Paris-Saclay, INRAE, AgroParisTech, UMR SayFood, 91120 Palaiseau, France

7 <sup>b</sup>Université Paris-Saclay, INRAE, AgroParisTech, Micalis Institute, 78352 Jouy-en-Josas,  
8 France

9

10 Running Head: Viral dynamics and persistence on the cheese surface

11

12 #Address correspondence to Eric Dugat-Bony, [eric.dugat-bony@inrae.fr](mailto:eric.dugat-bony@inrae.fr).

13 \*Present address: Université de Paris Cité, INSERM, IAME, UMR 1137, 75018 Paris, France

14 **ABSTRACT**

15 The surface of smear-ripened cheeses constitutes a dynamic microbial ecosystem resulting from the  
16 successive development of different microbial groups. Recent studies indicate that a viral community,  
17 mainly composed of bacteriophages, coexists with cellular microorganisms in this ecosystem, but its  
18 ecological significance remains to be elucidated. In this work, we studied a French smear-ripened  
19 cheese by both viral metagenomics and 16S metabarcoding approaches to assess both the dynamics of  
20 phages and bacterial communities on the cheese surface during the ripening period, and their  
21 persistence in ready-to-eat cheeses over the years of production. We observed a clear transition of the  
22 phage community structure during ripening with a decreased relative abundance of viral species  
23 (vOTUs) associated with *Lactococcus* phages, which were replaced by vOTUs associated with phages  
24 infecting ripening bacteria such as *Brevibacterium*, *Glutamicibacter*, *Pseudoalteromonas* and *Vibrio*.  
25 The dynamics of the phage community was strongly associated with bacterial successions observed on  
26 the cheese surface. Finally, a core of abundant vOTUs were systematically detected in ready-to-eat  
27 cheeses produced at different dates spanning more than 4 years of production, indicating long-term  
28 persistence of the main phages in the cheese production environment. Together, these findings offer  
29 novel perspectives on the ecology of bacteriophages in smear-ripened cheese and emphasize the  
30 significance of incorporating bacteriophages in the microbial ecology studies of fermented foods.

31 **IMPORTANCE**

32 Smear-ripened cheeses are microbial ecosystems made up of various microorganisms including  
33 bacteria, yeasts and also viruses such as bacteriophages, which infect and regulate bacterial  
34 populations. In this work, a French smear-ripened cheese was used to study how these viruses and  
35 bacteria interact over time and during cheese production. It revealed that the composition of the  
36 bacteriophage community shifts during the ripening process, aligning with the bacterial successions  
37 observed on the cheese surface between lactic acid bacteria and ripening bacteria. Additionally, the  
38 vast majority of these bacteriophages were found consistently in cheese products made over a 4-years  
39 period, showing that they represent a persistent component of the cheese-making environment. This  
40 research highlights the importance of considering these bacteriophages when studying the microbial  
41 life of fermented foods like cheese.

42

## 43 INTRODUCTION

44 Due to their unique ripening process, involving frequent washes with saline and/or alcoholic solutions,  
45 smear-ripened cheeses host a peculiar and diverse microbiota composed of lactic acid bacteria (LAB,  
46 mainly starter cultures added at the beginning of the process for milk acidification), yeasts and salt-  
47 tolerant bacteria belonging to the Actinomycetota, Bacillota and Pseudomonadota phyla (1). The  
48 surface microbiota of smear-ripened cheeses is considered to be responsible for the typical flavour and  
49 organoleptic properties of this type of cheese (2). From the past two decades, numerous studies have  
50 been conducted to describe the composition of this microbiota using isolation-based methods (3, 4),  
51 molecular fingerprinting (5–8), and more recently amplicon-based metagenomics also commonly  
52 referred to as metabarcoding (9–12).

53 Time series studies also enabled to reveal microbial successions occurring on the surface of smear-  
54 ripened cheeses during the maturation process (8, 13). Lactic acid bacteria (LAB), usually originating  
55 from starter cultures, grow first in the milk and represent the dominant microorganisms in the curd.  
56 Yeasts, *e.g. Debaryomyces hansenii* and *Geotrichum candidum*, which exhibit acid tolerance and  
57 metabolize lactate, subsequently colonize the cheese surface, resulting in its deacidification. With the  
58 pH increase, the establishment of a diverse bacterial community is progressively observed. The most  
59 common bacterial taxa detected at the end of ripening on smear-ripened cheese belong to coryneform  
60 bacteria (*e.g.* species of the *Glutamicibacter*, *Brevibacterium*, *Corynebacterium* or *Brachybacterium*  
61 genera), *Staphylococcus* species and halophilic or halotolerant gram-negative bacteria (*e.g.* species of  
62 the *Psychrobacter*, *Halomonas*, *Pseudoalteromonas*, *Hafnia*, *Vibrio*, *Pseudomonas* or *Proteus* genera)  
63 (14).

64 Microbial interactions are key biotic factors determining the structure and functioning of cheese  
65 microbial ecosystems and, ultimately, affecting cheese quality and safety (15, 16). In many natural  
66 ecosystems, bacteriophage infections shapes the composition of bacterial populations (17) and recent  
67 work suggests the same applies to fermented foods (18, 19). In the dairy industry, the impact of LAB  
68 phages is well documented because their lytic activity can disturb the milk acidification step, causing

69 delay in the production and even total loss of production (20, 21). Consequently, the most studied  
70 dairy phages are *Lactococcus*, *Streptococcus*, *Lactobacillus* and *Leuconostoc* phages, infecting the  
71 main starter cultures (22). Viral metagenomics has been recently employed to characterize the  
72 bacteriophage communities in dairy samples, including whey (23) and cheeses (24, 25). These  
73 investigations have demonstrated that such viral communities are not restricted to LAB phages, but  
74 encompass a diverse array of phages that could potentially also infect non-inoculated and ripening  
75 bacteria during cheese production.

76 However, only few studies report the isolation of such virulent phages from cheese infecting ripening  
77 bacteria, *i.e.* *Propionibacterium freudeunreichii* and *Brevibacterium aurantiacum* (26–28). We also  
78 isolated in a previous work five new virulent phages, targeting *Glutamicibacter arilaitensis*,  
79 *Brevibacterium aurantiacum*, *Psychrobacter aquimaris* and *Leuconostoc falkenbergense*, from the  
80 surface of a French smear-ripened cheese suggesting that predation is likely to occur on such  
81 ecosystems for most of the dominant bacteria (29). However, little is known about their ecology. In  
82 this study, our aim was to enhance our understanding of the temporal distribution of bacteriophages  
83 and their bacterial hosts on the surface of a French smear-ripened cheese across two distinct time  
84 scales. Initially, cheeses were obtained directly from the production facility at five distinct ripening  
85 stages over 28 days, to analyze phage dynamics throughout a production cycle (Figure 1, dynamic  
86 study). Subsequently, ready-to-eat cheeses of the same brand and variety were sampled in 2017, 2019,  
87 and 2022 to assess the long-term persistence of phages in this ecosystem (persistence study).

88

## 89 **RESULTS**

### 90 **Composition of the cheese surface virome.**

91 The sequence assembly obtained from all the studied samples (15 from the dynamic study and 9 from  
92 the persistence study) led to the production of a metavirome composed of 331 vOTUs >2 Kb (Table  
93 1). The vast majority of these contigs (284) were detected in samples from both the dynamic and  
94 persistence studies.

95 The most abundant phages detected in the dataset were identified as *Lactococcus* phages from the 949  
96 and 936 groups (*Audreyjarvisvirus* and *Skunavirus* genera, respectively) and *Glutamicibacter* phage

97 Montesquieu (Table 2). Of importance, the five virulent phages previously isolated from the same  
98 cheese, namely Montesquieu, Voltaire, Rousseau, D'Alembert and Diderot were also detected in this  
99 metagenomics survey. Remarkably, the vOTUs with no match (BLAT identity  $\times$  coverage  $<$  30%) to  
100 any known dairy phages (Table S1) represented only 3% of the relative abundance in the dataset,  
101 showing that most of the dominant phages present in this ecosystem have already close-relatives that  
102 have been isolated and characterized.

103 **The composition of the viral community present on the cheese surface evolves through the**  
104 **ripening process.**

105 The effect of each production step on the cheese virome composition was assessed by computing  
106 Bray-Curtis dissimilarity (BC). The PERMANOVA test indicated a significant effect of this variable  
107 ( $p$ -value = 0.001,  $R^2=0.658$ ) and the principal coordinate analysis revealed that the first axis clearly  
108 discriminates samples from the first 3 washes (NaCl) and samples from the two last washes (NaCl +  
109 alcoholic liquor) (Figure 2A). The second axis helps discriminating samples from the third wash (W3)  
110 and samples from the two first (W1 and 2). Regarding the viral diversity, as estimated by the Shannon  
111 index, a slight decrease was noted from W3 onwards. However, this decrease was not statistically  
112 significant, suggesting that there were no major alterations of the viral diversity related to the  
113 production step ( $p>0.05$ , Kruskal-Wallis test; Figure 2B).

114 In order to visualize the abundance of the different vOTUs in the samples, we kept only those with a  
115 normalized relative abundance above  $5 \times 10^{-5}$  in average (168 contigs) and represented their distribution  
116 across samples through a heatmap (Figure 2C). Three blocks of vOTUs were detected. The first one  
117 (top of the figure) was characterized by contigs whose abundance do not vary with the ripening and  
118 that corresponded mainly to virulent *Lactococcus* phages belonging to the 936 group (*Skunavirus*  
119 genus). The second block (bottom of the figure) contained contigs whose abundance decreased with  
120 ripening and that corresponded to other *Lactococcus* phages, close to the P335 group containing both  
121 temperate and virulent members (here qualified as ex-temperate phages). Finally, the third block  
122 (middle of the figure) was essentially composed of a few vOTUs that increased in relative abundance  
123 with ripening. These mainly corresponded to phages targeting ripening bacteria such as  
124 *Brevibacterium*, *Glutamicibacter*, *Pseudoalteromonas* and *Vibrio*, and non-starter lactic acid bacteria

125 (NSLAB) such as *Leuconostoc*. These few vOTUs correspond to uncharacterized phages, except  
126 *Glutamicibacter* phage Montesquieu, *Brevibacterium* phage Rousseau and *Leuconostoc* phage Diderot  
127 which we previously isolated from the same type of cheese.

128 As observed by the principal coordinate analysis of the Bray-Curtis dissimilarity (Figure 2A), the  
129 virome composition was similar between samples from W1 and W2, and between samples from W4  
130 and W5 indicating the presence of two main viral communities, according to these two ripening  
131 stages. Samples from W3 exhibited a composition in between samples from W1-2 and W4-5 reflecting  
132 a transition stage captured in those samples.

### 133 **Phage community shift during ripening follows changes in bacterial composition.**

134 We then applied the DESeq2 method to identify differentially abundant viral contigs between the two  
135 stable stages represented by W1-2 and W4-5 samples (Figure 3A). Interestingly, two groups emerged,  
136 with very readable outlines: vOTUs corresponding to phages infecting starter cultures, such as  
137 *Lactococcus* and *Streptococcus* phages, had a negative log<sub>2</sub> fold change meaning their relative  
138 abundances significantly decreased during the ripening process. Conversely, vOTUs of virulent  
139 phages targeting NSLAB and ripening bacteria (e.g. *Brevibacterium*, *Glutamicibacter*,  
140 *Pseudoalteromonas* and *Vibrio*) were significantly more abundant in W4-5 samples compared to W1-2  
141 samples (positive log<sub>2</sub> fold change) reflecting a higher population level for such phages on the cheese  
142 surface in later ripening stages. Among them were two vOTUs with high similarity to the genomes of  
143 *Glutamicibacter* phage Montesquieu (2017-3\_NODE2; 47,703 bp; 100% identity × coverage by  
144 BLAT), and *Brevibacterium* phage Rousseau (2022-5\_NODE4; 41,077 bp; 54% identity × coverage  
145 by BLAT but 98% identity at the nucleotidic level over a portion of >9 kb). In this group, we also  
146 detected a vOTU partially related to *Brevibacterium* phage AGM1 (SA2-0\_NODE10; 37148 bp; 3.5%  
147 identity × coverage by BLAT but 88% identity at the nucleotidic level over a portion of 1324 nt),  
148 which was isolated from a Canadian washed-rind cheese.

149 The composition of the bacterial community of the cheese surface also varied through the ripening  
150 process (Figure 3B). As for the virome composition, we observed a clear transition in the bacterial  
151 community structure from W3 onwards. *Lactococcus* was the dominant genus in samples from W1  
152 and W2, and was progressively replaced by typical surface aerobic bacteria such as members of

153 *Psychrobacter*, *Vibrio*, *Glutamicibacter* and *Pseudoalteromonas* genera. Based on plate counts (Figure  
154 3 C-E), this results should be mainly attributed to the growth of aerobic bacteria (~ 2 logs increase  
155 between W1 and W5, from ~  $10^8$  to ~  $10^{10}$  CFU/g) since lactic acid remained stable over time (~  $10^8$   
156 CFU/g) during the whole kinetic. This shift indicates that changes observed on the phage community  
157 structure is strongly associated with bacterial successions on the cheese surface.

### 158 **The dominant fraction of the cheese virome persists across production years.**

159 The effect of the production year (2017, 2019 and 2022) on the composition of the virome of the  
160 cheese surface (ready-to-eat cheeses, meaning after packaging and storage) was assessed by  
161 computing Bray-Curtis dissimilarity (Figure 4A). The PERMANOVA test indicated a significant  
162 effect of this factor (p-value of 0.002,  $R^2 = 0.814$ ) suggesting structural variations of the phage  
163 community across production years. The principal coordinate analysis revealed that the first axis  
164 clearly discriminates 2019 samples from 2017 and 2022 samples. The second axis helps discriminating  
165 samples from years 2017 and 2022.

166 The heatmap visualization showed that the vast majority of the most abundant contigs were shared  
167 among the 3 production years and that only a few low-abundant contigs were detected specifically in  
168 one or two production years (blue zones on the graph) (Figure 4C). This result is congruent with the  
169 stability of the bacterial community composition over the three sampling campaigns (Figure 4B).

170 We then evaluated the proportion of vOTUs that were shared across production year. When using the  
171 complete dataset (no filtering on relative abundance, Figure 4D), we observed that 56.6% of the 297  
172 vOTUs present in at least one of the three years were shared in all production years (75.4% in two  
173 different production years). Interestingly, samples from year 2022 had a higher number of unique  
174 vOTUs (48, 32.1% of the total) than samples from years 2017 and 2019 (3 and 11, respectively). We  
175 next applied the same analysis only on the most abundant vOTUs (average normalized relative  
176 abundance  $> 5 \times 10^{-5}$ , 99 vOTUs in total) (Figure 4E). The vast majority of the vOTUs, *i.e.* 89.9%,  
177 were shared among the 3 productions years and this value rose to 97% when considering only two  
178 different years. This result indicates that the cheese surface virome was mostly stable in terms of  
179 composition (presence/absence) and that dominant phages persist across productions years. The  
180 disparity between production years, as detected by beta-diversity analysis, may therefore primarily be

181 attributed to the presence or absence of phages in low abundance, and fluctuations in the relative  
182 abundance of dominant phages.

183

## 184 **DISCUSSION**

185 Recent studies of cheese samples using viral metagenomics (24, 25) or exploration of cheese microbial  
186 metagenomes (30) have revealed that the cheese environment harbours a diverse bacteriophage  
187 community whose targets go beyond lactic acid starter cultures. The isolation of a few representatives  
188 of these non-starter phages (27–29) suggests that phage activity occurs in this ecosystem, raising the  
189 question of their overall impact on microbial successions during the ripening process. Recently, the  
190 deliberate addition of one of those phages, *Brevibacterium* phage AGM9, was proven to slow down  
191 the development of the orange rind color in a model system mimicking a smear-ripened cheese (31). In  
192 the present study, we described the viral community of a French smear ripened cheese over time, by  
193 combining two timescales: the 28-days long ripening process, as well as from ready-to-eat cheeses  
194 spanning four years of production. The virome was predominantly composed of vOTUs associated  
195 with a variety of *Lactococcus* phages as well as the *Glutamicibacter* phage Montesquieu, a virulent  
196 phage we had previously isolated from the same cheese variety (29). This phage targets the ripening  
197 bacterium *Glutamicibacter arilaitensis*. Several other phages were detected at sub-dominant levels.  
198 Among them, only a few, such as the *Brevibacterium* phage Rousseau, *Leuconostoc* phage Diderot,  
199 *Psychrobacter* phage d’Alembert, *Glutamicibacter* phage Voltaire, and a novel vOTU displaying  
200 minimal sequence homology to *Brevibacterium* phage AGM1, have been previously documented in  
201 cheese. The diversity of these sub-dominant phages is therefore not yet completely sampled and, in  
202 particular, underscores the necessity to isolate a more comprehensive collection of phages from this  
203 ecosystem. Notably, we identified vOTUs that partially aligned with genomic sequences from phages  
204 infecting halotolerant bacteria (e.g., *Pseudoalteromonas*, *Halomonas*, *Vibrio*, and *Proteus* species).  
205 Even though these bacteria are not intentionally inoculated into smear-ripened cheese, they tend to  
206 dominate by the end of the ripening process (14). Their phages should therefore be looked for in future  
207 isolation initiatives.

208 The dynamics of bacterial and fungal communities has been extensively studied in a wide diversity of  
209 cheese products during ripening (13, 32–36), enabling to accurately describe cellular successions  
210 occurring in cheese production processes (16). In this study, we present the first analysis of viral  
211 dynamics throughout cheese ripening. Similar to the observed transitions in bacteria and fungi, there  
212 was a distinct shift in viral composition over the course of the ripening process. Some vOTUs  
213 associated with LAB starter-phages, primarily targeting *Lactococcus lactis*, were progressively  
214 replaced by vOTUs specific to phages that infect ripening bacteria. When comparing phage to  
215 bacterial dynamics, there was a notable relationship between phage trajectories and bacterial  
216 successions on the cheese surface. Specifically, the relative abundance of phages exhibited a  
217 concomitant increase with the relative abundance of their predicted bacterial hosts. This findings is of  
218 importance since the increase in the relative abundance of a specific vOTU within a virome can be  
219 interpreted as indicative of the active replication of the corresponding phage and further suggests the  
220 presence of a predator-prey interaction within the investigated ecosystem.

221 Surprisingly, despite the changes in bacterial and viral communities' composition during the  
222 production process, the relative abundance of some vOTUs remained very stable during ripening.  
223 They mainly corresponded to virulent *Lactococcus* phages, belonging to the *Skunavirus* genus  
224 (formerly 936 group). Among *Lactococcus* phages, this genus is by far the most frequently detected in  
225 the dairy industry (37). Given that *Lactococcus lactis* predominantly proliferates during milk  
226 acidification and maintains consistent concentration levels throughout the ripening period in this type  
227 of cheese (13), we theorize that the maintenance of *Skunavirus* is indicative of the stability of phage  
228 particles produced at the onset of cheese maturation. The remarkable stability of *Skunavirus* particles  
229 in comparison to other *Lactococcus* phage groups, especially the P335 group, has been reported earlier  
230 (38, 39). In contrast, we suggest that the relative decline observed in our experiment for certain  
231 *Lactococcus* phages, specifically those affiliated to the P335 group, denotes their temporal instability.  
232 Nevertheless, a more comprehensive examination of this phenomenon warrants dedicated  
233 investigations.

234 Cheese microbial communities of washed-rind cheese are generally dominated by environmental  
235 microorganisms detected in processing environments, the so-called “house” microbiota (40), which is  
236 specific to each production facility and provides a microbial signature distinguishing cheeses  
237 belonging to the same variety but manufactured by distinct producers (10). Recently, the analysis of  
238 several Quebec’s terroir cheeses revealed that the dominant microorganisms remain stable from year  
239 to year, which could be linked to typical manufacturing practices and consistency in the use of starter  
240 and ripening cultures by cheesemakers (41). Here, we describe a similar observation for  
241 bacteriophages. We indeed identified a core-virome composed of a large proportion of the most  
242 abundant vOTUs, consistently detected across four production years. Previous work on an undefined  
243 starter culture used for the production of a Swiss-type cheese, propagated for decades in the same  
244 dairy environment, revealed that phages and bacteria stably coexist over time in this system and  
245 suggests that this may contribute to the stable maintenance of the cheese starter culture over years  
246 (42). The same may apply for phages and bacteria on the surface of smear-ripened cheese since both  
247 are contaminating the cheese production environment, and are therefore likely to repeatedly  
248 contaminate cheese from one production cycle to another (29, 40).

249 In conclusion, the observed dynamics of the cheese virome throughout the ripening process, coupled  
250 with its relative persistence across production years, support an important role of bacteriophages in the  
251 cheese microbial ecosystem. Recognizing this biotic factor is essential for a comprehensive  
252 understanding of microbial successions during milk fermentation. Moreover, this knowledge may  
253 offer cheesemakers novel avenues to refine and control their production processes.

254

## 255 **MATERIAL AND METHODS**

### 256 **Cheese samples.**

257 (i) Dynamic study design: French smear-ripened cheeses, all from the same production batch, were  
258 collected directly from the cheese plant at five different stages during the ripening process (Figure 1).  
259 These stages, labeled W1 to W5, correspond to distinct washing steps. The initial three washes utilized  
260 a NaCl solution, while the final two employed a NaCl solution supplemented with increasing

261 concentrations of alcoholic liquor. At each stage, three distinct cheeses were sampled and designated  
262 as replicates A, B, and C. Cheeses were immediately stored at 4°C after sampling and processed  
263 within 48h.

264 (ii) Persistence study design: ready-to-consume cheeses of the same type and same brand as the  
265 previously described cheeses were purchased in a local supermarket in December 2017, November  
266 2019 and February 2022, spanning >4 years of production. Three different cheeses, with the same  
267 production date, were sampled each year and used as replicates. Cheeses were immediately stored at  
268 4°C after sampling and processed within 48h.

269 For both dynamic and persistence studies, cheese samples were analysed immediately after reception  
270 at the lab. Using sterile knives, the rind, approximately 2-3 mm thick, was carefully separated from the  
271 core. It was then blended and processed for microbial counts, viral DNA extraction for metavirome  
272 analysis, and microbial DNA extraction for extensive amplicon sequencing targeting the 16S rRNA  
273 gene, which will be subsequently referred to as 16S metabarcoding.

#### 274 **Microbiological analysis.**

275 Bacteria and yeasts were enumerated by plating serial dilutions ( $10^{-1}$  to  $10^{-7}$ ) of one gram of cheese  
276 rind mixed in 9 mL of physiological water (9 g/L NaCl) on three different culture media. Brain Heart  
277 Infusion Agar (BHI, Biokar Diagnostics) supplemented with 50 mg/L amphotericin (Sigma Aldrich,  
278 Saint-Louis, MO, USA) was used to count total aerobic bacteria after 48 h of incubation at 28°C. Man,  
279 Rogosa and Sharpe Agar (MRS, Biokar Diagnostics, Allonne, France) supplemented with 50 mg/L  
280 amphotericin was used to count lactic acid bacteria after 48 h of incubation at 30°C under anaerobic  
281 conditions. Yeasts were counted on Yeast Extract Glucose Chloramphenicol (YEGC, Biokar  
282 Diagnostics, Allonne, France) after 48 h of incubation at 28°C.

#### 283 **Viral DNA extraction and metavirome analysis.**

284 Extraction of the viral fraction from cheese rind was performed according to protocol P4 detailed in  
285 (24) comprising a filtration step and a chloroform treatment. DNA was extracted from the viral  
286 particles according to the protocol described in the same study and sent to Eurofins Genomics for high  
287 throughput sequencing using the Illumina NovaSeq platform ( $2 \times 150$  bp paired-end reads,  
288 approximately 10 million reads per sample).

289 All the details about the tools, versions and parameters used in the following pipeline are available in  
290 scripts deposited in the GitLab repository ([https://forgemia.inra.fr/eric.dugat-bony/cheese\\_virome](https://forgemia.inra.fr/eric.dugat-bony/cheese_virome)).  
291 Briefly, raw reads were quality filtered using Trimmomatic v0.39 (43). Then a single assembly was  
292 computed for the collection of triplicate reads from each sample with Spades v3.15.3 (44), using either  
293 the complete dataset of trimmed reads available or after subsampling the dataset to 1.5 million,  
294 150,000 or 15,000 trimmed reads per sample. We noted that some abundant contigs were assembled  
295 into longer, nearly complete contigs, after subsampling. Contigs of length >2kb from all assemblies  
296 were selected and clustered following an approach adapted from (45). Succinctly, a pairwise alignment  
297 was first performed for all contigs using BLAT (46). Then, contigs with a self-alignment > 110% of  
298 contig length, corresponding to chimeras, were removed. Remaining contigs were clustered at the  
299 species level (90% identity × coverage) and the longest contig within each cluster was selected as the  
300 representative sequence. The final contig dataset consisted in 3122 dereplicated contigs.

301 Viral contigs were selected using a combination of three detection tools: VIBRANT v1.2.1 (47),  
302 VirSorter2 v2.2.4 (48) and CheckV v0.8.1 (49). The ones retained in the final virome were those  
303 meeting at least one of the following criteria: declared “complete”, “high” or “medium” quality by  
304 either VIBRANT or CheckV, declared “full” by VirSorter2. The bacterial host of the 332 viral contigs  
305 was predicted using iPHoP (50). Finally, all sequences were compared by BLAT to an in-house  
306 database consisting of genome sequences from 32 common dairy phages (listed in Table S1) in order  
307 to identify potential related phages with known taxonomy, verified host and lifestyle (30% identity ×  
308 coverage minimal cutoff). When appropriate, the host genus predicted by iPHoP was replaced by the  
309 genus of the bacterial host of the closest relative phage identified by the BLAT search. One contig,  
310 corresponding to the genome of the phage PhiX174 which is routinely used as control in Illumina  
311 sequencing runs to monitor sequencing quality, was discarded resulting in a final dataset of 331 viral  
312 contigs.

313 In order to evaluate the relative abundance of each viral contig in each metavirome sample, trimmed  
314 reads were mapped against the viral contigs using bwa-mem2 v2.2.1 (51) and counted with Msamtools  
315 v1.0.0 profile with the options --multi=equal --unit=ab -nolen  
316 (<https://github.com/arumugamlab/msamtools>). The output files from all samples were joined into an

317 abundance table and processed using the R package phyloseq v1.38.0 (52). For each experimental  
318 dataset (dynamic study, persistence study), read counts were rarefied to the minimum depth observed  
319 in one individual sample. Then, read counts were normalized by contig length and transformed to  
320 relative abundances, in order to enable both comparison of the viral community structure between  
321 samples and comparison of the abundance level between contigs. Making the assumption that one  
322 viral contig corresponds to one species (which is wrong each time several contigs belonging to the  
323 same phage genome are present), Bray-Curtis dissimilarity index, as computed by the distance  
324 function from the R package phyloseq, was used to compare viral communities between samples and  
325 the effect of different variables on their structure was assessed using permutational analysis of  
326 variance as computed by the adonis2 function from the R package vegan v2.6-2.

327 For the dynamic dataset, differential analysis was performed on raw counts using the DESeq function  
328 implemented in the DESeq2 package v1.38.0 (53). Indeed, this function already includes a  
329 normalization step (by the median of ratios method). Contigs were considered differentially abundant  
330 if adjusted pvalue > 0.01, log2 fold change > 3 or < -3 and average raw counts > 1500.

### 331 **Microbial DNA extraction and 16S metabarcoding profiles.**

332 Total DNA extraction from the cheese surface was performed as previously described (10). PCR  
333 amplification of the V3-V4 regions of the 16S rRNA gene was performed with the primers V3F (5'-  
334 ACGGRAGGCWGCAG-3') and V4R (5'-TACCAGGGTATCTAATCCT-3')  
335 carrying the Illumina 5'-CTTCCCTACACGACGCTCTTCCGATCT-3' and the 5'-  
336 GGAGTTCAGACGTGTGCTCTTCCGATCT-3' tails, respectively. The reaction was performed  
337 using 10 ng of extracted DNA, 0.5  $\mu$ M primer, 0.2 mM dNTP, and 2.5 U of the MTP Taq DNA  
338 polymerase (Sigma-Aldrich, USA). The amplification was carried out using the following program:  
339 94°C for 60 s, 30 cycles at 94°C for 60 s, 65°C for 60 s, 72°C for 60 s, and a final elongation step at  
340 72°C for 10 min. The resulting PCR products were sent to the @BRIDGE platform (INRAE, Jouy-en-  
341 Josas, France) for library preparation and sequencing. Briefly, amplicons were purified using a  
342 magnetic beads CleanPCR (Clean NA, GC biotech B.V., The Netherlands), the concentration was  
343 measured using a Nanodrop spectrophotometer (Thermo Scientific, USA) and the amplicon quality  
344 was assessed on a Fragment Analyzer (AATI, USA) with the reagent kit ADNdb 910 (35-1,500 bp).

345 Sample multiplexing was performed by adding tailor-made 6 bp unique indexes during the second  
346 PCR step which was performed on 50–200 ng of purified amplicons using the following program:  
347 94°C for 10 min, 12 cycles at 94°C for 60 s, 65°C for 60 s, 72°C for 60 s, and a final elongation step at  
348 72°C for 10 min. After purification and quantification (as described above), all libraries were pooled  
349 with equal amounts in order to generate equivalent number of raw reads for each library. The DNA  
350 concentration of the pool was quantified on a Qubit Fluorometer (ThermoFisher Scientific, USA) and  
351 adjusted to a final concentration between 5 and 20 nM for sequencing. The pool was denatured (NaOH  
352 0.1N) and diluted to 7 pM. The PhiX Control v3 (Illumina, USA) was added to the pool at 15% of the  
353 final concentration, as described in the Illumina procedure, and the mixture was loaded onto the  
354 Illumina MiSeq cartridge according to the manufacturer's instructions using MiSeq Reagent Kit v3 (2  
355 × 250 bp paired-end reads).

356 Paired-end reads were analysed using FROGS v3.2 (54), according to the standard operating  
357 procedure. Briefly, operational taxonomic units (OTUs) were built using Swarm with an aggregation  
358 distance of 1 and the --fastidious option (55), and each OTU that accounted for <0.005% of the total  
359 dataset of sequences was discarded, as previously recommended (56). Lastly, the OTU's affiliation  
360 was checked using the EzBiocloud database v52018 (57). The abundance table was processed using  
361 the R package phyloseq v1.38.0 (52).

#### 362 **Data availability.**

363 Raw sequencing data for cheese virome and bacterial microbiome were deposited at the sequence read  
364 archive (SRA) of the NCBI (<https://www.ncbi.nlm.nih.gov/sra/>) as part of bioprojects PRJNA984302  
365 (dynamic study) and PRJNA984735 (persistence study).

366

#### 367 **ACKNOWLEDGMENTS**

368 T.P. is the recipient of a doctoral fellowship from the French Ministry of Higher Education, Research  
369 and Innovation (MESRI) and the MICA department of the French National Research Institute for  
370 Agriculture, Food and Environment (INRAE). For the metabarcoding analysis, this work has benefited  
371 from the facilities and expertise of @BRIDGE (Université Paris-Saclay, INRAE, AgroParisTech,  
372 GABI, 78350 Jouy-en-Josas, France). We are also grateful to the INRAE MIGALE bioinformatics

373 facility (MIGALE, INRAE, 2020. Migale bioinformatics Facility, doi:  
374 10.15454/1.5572390655343293E12) for providing computing and storage resources.

375

376 **TABLES**

377 **Table 1: summary statistics about the metavirome dataset.**

|   | <b>Complete dataset<br/>(24 samples)</b> | <b>Dynamic<br/>study (15<br/>samples)</b> | <b>Persistence<br/>study (9<br/>samples)</b> |
|---|--|---|--|
| <b>Total number of vOTUs &gt; 2 Kb</b>  | 331                                      | 318                                       | 297  |
| <b>Number of vOTUs with relative<br/>abundance &gt; <math>5 \times 10^{-5}</math></b> | 157                                      | 168                                       | 99   |

378

379 **Table 2: Most abundant dairy phages detected on the cheese metavirome.** Phages that have been  
380 previously isolated from the same cheese variety are highlighted in bold. When classification is  
381 available at the International Committee on Taxonomy of Viruses (ICTV), the viral genus is denoted  
382 in brackets.

| <b>Closest relatives</b>                                  | <b>Relative abundance*</b> |
|---|----------------------------|
| <i>Lactococcus</i> 949 group ( <i>Audreyjarvisvirus</i> ) | 0.56                       |
| <b><i>Glutamicibacter</i> Montesquieu</b>                 | <b>0.23</b>                |
| <i>Lactococcus</i> 936 group ( <i>Skunavirus</i> )        | 0.18                       |
| <i>Lactococcus</i> P335 group                             | 1.54E-03                   |
| <b><i>Brevibacterium</i> Rousseau</b>                     | <b>1.08E-03</b>            |
| <b><i>Psychrobacter</i> D'Alembert</b>                    | <b>1.74E-04</b>            |
| <b><i>Leuconostoc</i> Diderot (<i>Limdunavirus</i>)</b>   | <b>1.14E-04</b>            |
| <b><i>Glutamicibacter</i> Voltaire</b>                    | <b>1.70E-05</b>            |
| <i>Streptococcus</i> 987 group                            | 7.87E-06                   |

*Lactococcus* KSY1 group (*Chopinivirus*)

5.94E-07

Non dairy phages\*\*

0.03

383 \*The relative abundance value used here is not normalized by genome size, it corresponds to the  
384 relative proportion of reads mapping to all vOTUs belonging to a given phage group present in our in-  
385 house dairy phage database (Table S1).

386 \*\*vOTUs without any match to our in-house dairy phage database (30% identity  $\times$  coverage minimal  
387 cutoff).

388

### 389 **FIGURE LEGENDS**

390 **Figure 1: Schematic representation of the experimental plan followed for the dynamic study of**  
391 **the virome composition during the ripening process.** Samples were respectively obtained after each  
392 washing step (blue arrows indicate washes performed with a NaCl solution, red arrows indicate  
393 washes performed with a NaCl solution containing alcoholic liquor).

394

395 **Figure 2: Dynamic of the cheese surface virome along the ripening process.** A) Principal  
396 coordinate analysis of the Bray-Curtis dissimilarity. Samples are coloured according the ripening step.  
397 B) Comparison of the viral diversity, estimated by the Shannon index, at the different ripening steps.  
398 C) Heatmap representing the normalized relative abundance of the most abundant vOTUs present in  
399 the dataset (168 vOTUs with an averaged normalized relative abundance value  $5 \times 10^{-5}$ ) in the  
400 different samples. The colours on the heatmap represent the log-transformed relative abundance, and  
401 range from blue to red, blue indicating lower relative abundance and red indicating higher relative  
402 abundance. When available, vOTU annotations were indicated such as the host genus as predicted by  
403 iPHoP, the group of known phages it belongs to and its lifestyle.

404

405 **Figure 3: Relationship between phage dynamic and the composition of cheese bacterial**  
406 **community.** A) Differential abundance analysis on the virome data between the two stable stages  
407 represented by W1-2 and W4-5 samples. Log2 fold change values obtained for differential abundant

408 vOTUs (points) are represented and the dot colour indicate the predicted host genus according to  
409 iPHoP. Grey dots: no predicted host. B) Composition of the bacterial community assessed by a  
410 metabarcoding approach targeting the V3-V4 regions of the 16S rRNA gene. Three different cheeses  
411 from the same batch were analysed at each sampling point. Data were aggregated at the genus level.  
412 C) Yeasts counts expressed in log(CFU/g). D) Aerobic bacteria counts expressed in log(CFU/g). E)  
413 Lactic acid bacteria counts expressed in log(CFU/g).

414

415 **Figure 4: Persistence of the cheese surface virome across production years.** A) Principal  
416 coordinate analysis of the Bray-Curtis dissimilarity. Samples are coloured according the production  
417 year (2017, 2019 and 2022). B) Composition of the bacterial community assessed by a metabarcoding  
418 approach targeting the V3-V4 regions of the 16S rRNA gene. Three different cheeses from the same  
419 production year were analysed. Data were aggregated at the genus level. C) Heatmap representing the  
420 normalized relative abundance of the most abundant vOTUs (99 with an averaged normalized relative  
421 abundance value  $> 5 \times 10^{-5}$ ) in each sample. The colours on the heatmap represent the log-transformed  
422 relative abundance, and range from blue to red, blue indicating lower relative abundance and red  
423 indicating higher relative abundance. D) Venn diagram constructed from the dataset without filtering,  
424 comprising 297 vOTUs. E) Venn diagram constructed from the filtered dataset comprising 99 vOTUs  
425 with an averaged normalized relative abundance value  $> 5 \times 10^{-5}$ .

426

#### 427 **SUPPLEMENTARY MATERIAL**

428 **Table S1. Common dairy phages and associated information.**

429

#### 430 **REFERENCES**

- 431 1. Mounier J, Coton M, Irlinger F, Landaud S, Bonnarme P. 2017. Chapter 38 - Smear-Ripened  
432 Cheeses, p. 955–996. *In* McSweeney, PLH, Fox, PF, Cotter, PD, Everett, DW (eds.), *Cheese*  
433 (Fourth Edition). Academic Press, San Diego.

- 434 2. Corsetti A, Rossi J, Gobbetti M. 2001. Interactions between yeasts and bacteria in the smear  
435 surface-ripened cheeses. *International Journal of Food Microbiology* 69:1–10.
- 436 3. Larpin-Laborde S, Imran M, Bonaïti C, Bora N, Gelsomino R, Goerges S, Irlinger F, Goodfellow M,  
437 Ward AC, Vancanneyt M, Swings J, Scherer S, Guéguen M, Desmasures N. 2011. Surface  
438 microbial consortia from Livarot, a French smear-ripened cheese. *Canadian Journal of*  
439 *Microbiology* 57:651–660.
- 440 4. Lavoie K, Touchette M, St-Gelais D, Labrie S. 2012. Characterization of the fungal microflora in  
441 raw milk and specialty cheeses of the province of Quebec. *Dairy Sci & Technol* 92:455–468.
- 442 5. Feurer C, Irlinger F, Spinnler H e., Glaser P, Vallaëys T. 2004. Assessment of the rind microbial  
443 diversity in a farmhouse-produced vs a pasteurized industrially produced soft red-smear cheese  
444 using both cultivation and rDNA-based methods. *Journal of Applied Microbiology* 97:546–556.
- 445 6. Mounier J, Monnet C, Jacques N, Antoinette A, Irlinger F. 2009. Assessment of the microbial  
446 diversity at the surface of Livarot cheese using culture-dependent and independent  
447 approaches. *International Journal of Food Microbiology* 133:31–37.
- 448 7. Mounier J, Gelsomino R, Goerges S, Vancanneyt M, Vandemeulebroecke K, Hoste B, Scherer S,  
449 Swings J, Fitzgerald GF, Cogan TM. 2005. Surface Microflora of Four Smear-Ripened Cheeses.  
450 *Appl Environ Microbiol* 71:6489–6500.
- 451 8. Rea MC, Görges S, Gelsomino R, Brennan NM, Mounier J, Vancanneyt M, Scherer S, Swings J,  
452 Cogan TM. 2007. Stability of the Biodiversity of the Surface Consortia of Gubbeen, a Red-Smear  
453 Cheese. *Journal of Dairy Science* 90:2200–2210.
- 454 9. Delcenserie V, Taminiau B, Delhalle L, Nezer C, Doyen P, Crevecoeur S, Roussey D, Korsak N,  
455 Daube G. 2014. Microbiota characterization of a Belgian protected designation of origin cheese,  
456 Herve cheese, using metagenomic analysis. *Journal of Dairy Science* 97:6046–6056.

- 457 10. Dugat-Bony E, Garnier L, Denonfoux J, Ferreira S, Sarthou A-S, Bonnarme P, Irlinger F. 2016.  
458 Highlighting the microbial diversity of 12 French cheese varieties. *International Journal of Food*  
459 *Microbiology* 238:265–273.
- 460 11. Quigley L, O’Sullivan O, Beresford TP, Ross RP, Fitzgerald GF, Cotter PD. 2012. High-throughput  
461 sequencing for detection of subpopulations of bacteria not previously associated with artisanal  
462 cheeses. *Applied and Environmental Microbiology* 78:5717–5723.
- 463 12. Wolfe BE, Button JE, Santarelli M, Dutton RJ. 2014. Cheese rind communities provide tractable  
464 systems for in situ and in vitro studies of microbial diversity. *Cell* 158:422–433.
- 465 13. Irlinger F, Monnet C. 2021. Temporal differences in microbial composition of Époisses cheese  
466 rinds during ripening and storage. *Journal of Dairy Science* 104:7500–7508.
- 467 14. Kothe CI, Bolotin A, Kraïem B-F, Dridi B, Renault P. 2021. Unraveling the world of halophilic and  
468 halotolerant bacteria in cheese by combining cultural, genomic and metagenomic approaches.  
469 *International Journal of Food Microbiology* 358:109312.
- 470 15. Irlinger F, Mounier J. 2009. Microbial interactions in cheese: implications for cheese quality and  
471 safety. *Current Opinion in Biotechnology* 20:142–148.
- 472 16. Mayo B, Rodríguez J, Vázquez L, Flórez AB. 2021. Microbial Interactions within the Cheese  
473 Ecosystem and Their Application to Improve Quality and Safety. 3. *Foods* 10:602.
- 474 17. Brown TL, Charity OJ, Adriaenssens EM. 2022. Ecological and functional roles of bacteriophages  
475 in contrasting environments: marine, terrestrial and human gut. *Current Opinion in*  
476 *Microbiology* 70:102229.

- 477 18. Ledormand P, Desmasures N, Dalmasso M. 2020. Phage community involvement in fermented  
478 beverages: an open door to technological advances? *Critical Reviews in Food Science and*  
479 *Nutrition* 1–10.
- 480 19. Paillet T, Dugat-Bony E. 2021. Bacteriophage ecology of fermented foods: anything new under  
481 the sun? *Current Opinion in Food Science* 40:102–111.
- 482 20. Garneau JE, Moineau S. 2011. Bacteriophages of lactic acid bacteria and their impact on milk  
483 fermentations. *Microb Cell Fact* 10 Suppl 1:S20.
- 484 21. Pujato S a., Quiberoni A, Mercanti D j. 2019. Bacteriophages on dairy foods. *Journal of Applied*  
485 *Microbiology* 126:14–30.
- 486 22. Marcó MB, Moineau S, Quiberoni A. 2012. Bacteriophages and dairy fermentations.  
487 *Bacteriophage* 2:149–158.
- 488 23. Muhammed MK, Kot W, Neve H, Mahony J, Castro-Mejía JL, Krych L, Hansen LH, Nielsen DS,  
489 Sørensen SJ, Heller KJ, Sinderen D van, Vogensen FK. 2017. Metagenomic analysis of dairy  
490 bacteriophages: extraction method and pilot study on whey samples derived from using  
491 undefined and defined mesophilic starter cultures. *Appl Environ Microbiol* 83:e00888-17.
- 492 24. Dugat-Bony E, Lossouarn J, De Paepe M, Sarthou A-S, Fedala Y, Petit M-A, Chaillou S. 2020. Viral  
493 metagenomic analysis of the cheese surface: A comparative study of rapid procedures for  
494 extracting viral particles. *Food Microbiology* 85:103278.
- 495 25. Queiroz LL, Lacorte GA, Isidorio WR, Landgraf M, de Melo Franco BDG, Pinto UM, Hoffmann C.  
496 2022. High Level of Interaction between Phages and Bacteria in an Artisanal Raw Milk Cheese  
497 Microbial Community. *mSystems* 0:e00564-22.

- 498 26. Cheng L, Marinelli LJ, Grosset N, Fitz-Gibbon ST, Bowman CA, Dang BQ, Russell DA, Jacobs-Sera  
499 D, Shi B, Pellegrini M, Miller JF, Gautier M, Hatfull GF, Modlin RL. 2018. Complete genomic  
500 sequences of *Propionibacterium freudenreichii* phages from Swiss cheese reveal greater  
501 diversity than *Cutibacterium* (formerly *Propionibacterium*) *acnes* phages. *BMC Microbiology*  
502 18:19.
- 503 27. de Melo AG, Rousseau GM, Tremblay DM, Labrie SJ, Moineau S. 2020. DNA tandem repeats  
504 contribute to the genetic diversity of *Brevibacterium aurantiacum* phages. *Environmental*  
505 *Microbiology* 22:3413–3428.
- 506 28. Gautier M, Rouault A, Sommer P, Briandet R. 1995. Occurrence of *Propionibacterium*  
507 *freudenreichii* bacteriophages in swiss cheese. *Appl Environ Microbiol* 61:2572–2576.
- 508 29. Paillet T, Lossouarn J, Figueroa C, Midoux C, Rué O, Petit M-A, Dugat-Bony E. 2022. Virulent  
509 Phages Isolated from a Smear-Ripened Cheese Are Also Detected in Reservoirs of the Cheese  
510 Factory. 8. *Viruses* 14:1620.
- 511 30. Walsh AM, Macori G, Kilcawley KN, Cotter PD. 2020. Meta-analysis of cheese microbiomes  
512 highlights contributions to multiple aspects of quality. *Nat Food* 1:500–510.
- 513 31. de Melo AG, Lemay M-L, Moineau S. 2023. The impact of *Brevibacterium aurantiacum* virulent  
514 phages on the production of smear surface-ripened cheeses. *International Journal of Food*  
515 *Microbiology* 400:110252.
- 516 32. De Pasquale I, Di Cagno R, Buchin S, De Angelis M, Gobbetti M. 2014. Microbial Ecology  
517 Dynamics Reveal a Succession in the Core Microbiota Involved in the Ripening of Pasta Filata  
518 Caciocavallo Pugliese Cheese. *Applied and Environmental Microbiology* 80:6243–6255.

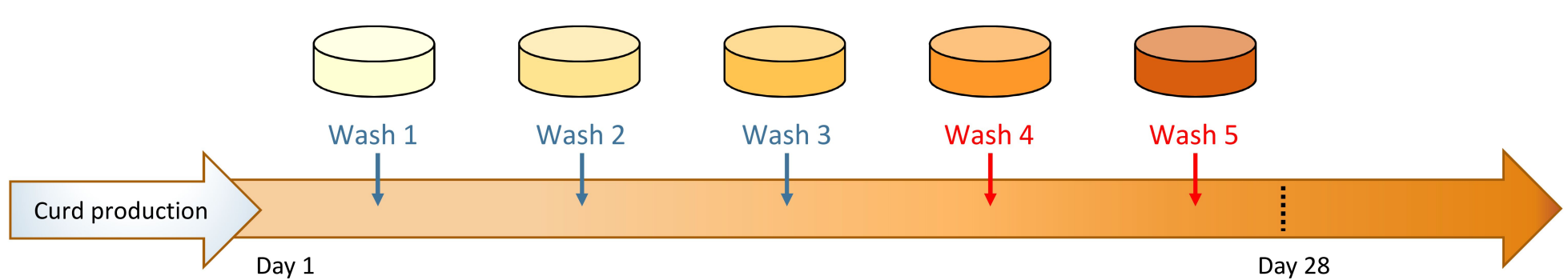
- 519 33. Flórez AB, Mayo B. 2006. Microbial diversity and succession during the manufacture and  
520 ripening of traditional, Spanish, blue-veined Cabrales cheese, as determined by PCR-DGGE.  
521 International Journal of Food Microbiology 110:165–171.
- 522 34. Fuka MM, Wallisch S, Engel M, Welzl G, Havranek J, Schloter M. 2013. Dynamics of Bacterial  
523 Communities during the Ripening Process of Different Croatian Cheese Types Derived from Raw  
524 Ewe’s Milk Cheeses. PLoS ONE 8:e80734.
- 525 35. Larpin S, Mondoloni C, Goerges S, Vernoux J-P, Guéguen M, Desmasures N. 2006. *Geotrichum*  
526 *candidum* dominates in yeast population dynamics in Livarot, a French red-smear cheese. FEMS  
527 Yeast Research 6:1243–1253.
- 528 36. Pangallo D, Šaková N, Koreňová J, Puškárová A, Kraková L, Valík L, Kuchta T. 2014. Microbial  
529 diversity and dynamics during the production of May bryndza cheese. International Journal of  
530 Food Microbiology 170:38–43.
- 531 37. Jolicoeur AP, Lemay M-L, Beaubien E, Bélanger J, Bergeron C, Bourque-Leblanc F, Doré L,  
532 Dupuis M-È, Fleury A, Garneau JE, Labrie SJ, Labrie S, Lacasse G, Lamontagne-Drolet M, Lessard-  
533 Hurtubise R, Martel B, Menasria R, Morin-Pelchat R, Pageau G, Samson JE, Rousseau GM,  
534 Tremblay DM, Duquenne M, Lamoureux M, Moineau S. 2023. Longitudinal Study of Lactococcus  
535 Phages in a Canadian Cheese Factory. Applied and Environmental Microbiology 0:e00421-23.
- 536 38. Madera C, Monjardín C, Suárez JE. 2004. Milk contamination and resistance to processing  
537 conditions determine the fate of Lactococcus lactis bacteriophages in dairies. Applied and  
538 Environmental Microbiology 70:7365–7371.
- 539 39. Wagner N, Brinks E, Samtlebe M, Hinrichs J, Atamer Z, Kot W, Franz CMAP, Neve H, Heller KJ.  
540 2017. Whey powders are a rich source and excellent storage matrix for dairy bacteriophages.  
541 International Journal of Food Microbiology 241:308–317.

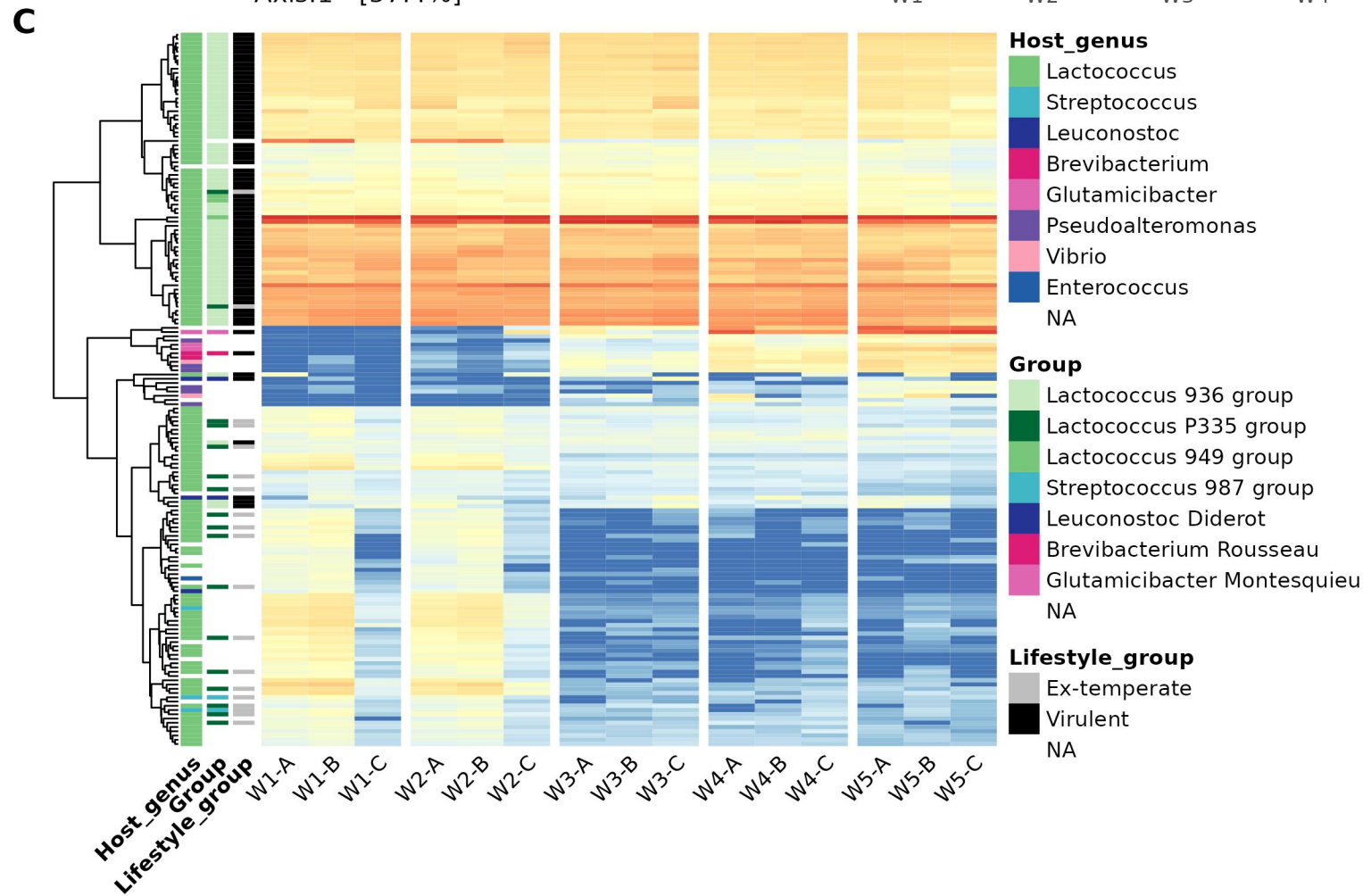
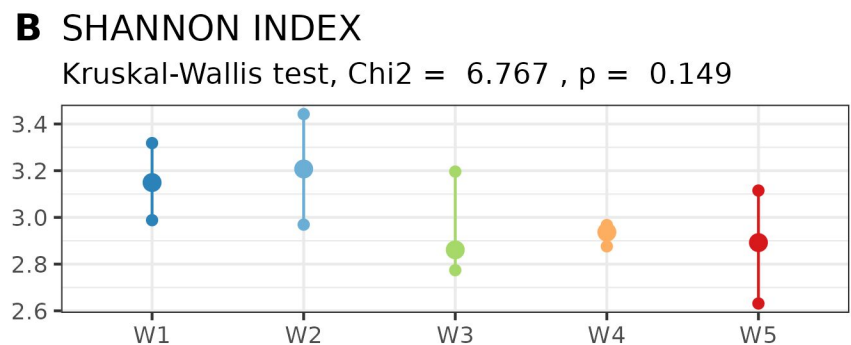
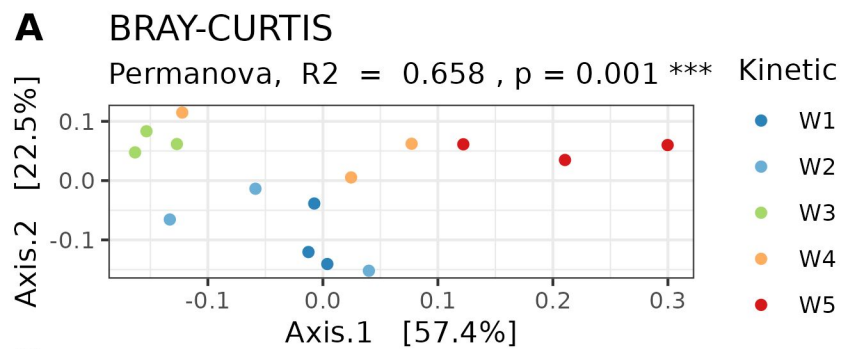
- 542 40. Bokulich NA, Mills DA. 2013. Facility-Specific “House” Microbiome Drives Microbial Landscapes  
543 of Artisan Cheesemaking Plants. *Applied and Environmental Microbiology* 79:5214–5223.
- 544 41. Raymond-Fleury A, Lessard M-H, Chamberland J, Pouliot Y, Dugat-Bony E, Turgeon SL, St-Gelais  
545 D, Labrie S. 2022. Analysis of Microbiota Persistence in Quebec’s Terroir Cheese Using a  
546 Metabarcoding Approach. *Microorganisms* 10:1381.
- 547 42. Somerville V, Berthoud H, Schmidt RS, Bachmann H-P, Meng YH, Fuchsmann P, von Ah U, Engel  
548 P. 2021. Functional strain redundancy and persistent phage infection in Swiss hard cheese  
549 starter cultures. *ISME J* 1–12.
- 550 43. Bolger AM, Lohse M, Usadel B. 2014. Trimmomatic: a flexible trimmer for Illumina sequence  
551 data. *Bioinformatics* 30:2114–2120.
- 552 44. Bankevich A, Nurk S, Antipov D, Gurevich AA, Dvorkin M, Kulikov AS, Lesin VM, Nikolenko SI,  
553 Pham S, Prjibelski AD, Pyshkin AV, Sirotkin AV, Vyahhi N, Tesler G, Alekseyev MA, Pevzner PA.  
554 2012. SPAdes: a new genome assembly algorithm and its applications to single-cell sequencing.  
555 *J Comput Biol* 19:455–477.
- 556 45. Shah SA, Deng L, Thorsen J, Pedersen AG, Dion MB, Castro-Mejía JL, Silins R, Romme FO,  
557 Sausset R, Jessen LE, Ndela EO, Hjelmsø M, Rasmussen MA, Redgwell TA, Leal Rodríguez C,  
558 Vestergaard G, Zhang Y, Chawes B, Bønnelykke K, Sørensen SJ, Bisgaard H, Enault F, Stokholm J,  
559 Moineau S, Petit M-A, Nielsen DS. 2023. Expanding known viral diversity in the healthy infant  
560 gut. *Nat Microbiol* 8:986–998.
- 561 46. Kent WJ. 2002. BLAT—The BLAST-Like Alignment Tool. *Genome Res* 12:656–664.
- 562 47. Kieft K, Zhou Z, Anantharaman K. 2020. VIBRANT: automated recovery, annotation and curation  
563 of microbial viruses, and evaluation of viral community function from genomic sequences.  
564 *Microbiome* 8:90.

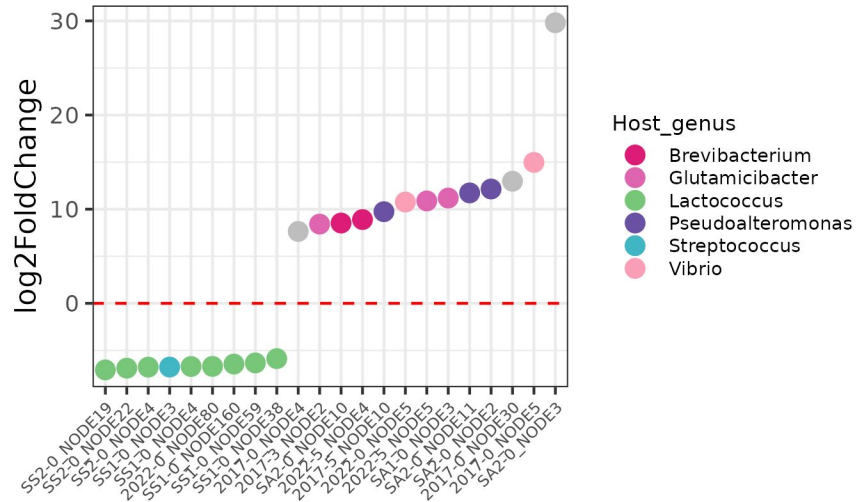
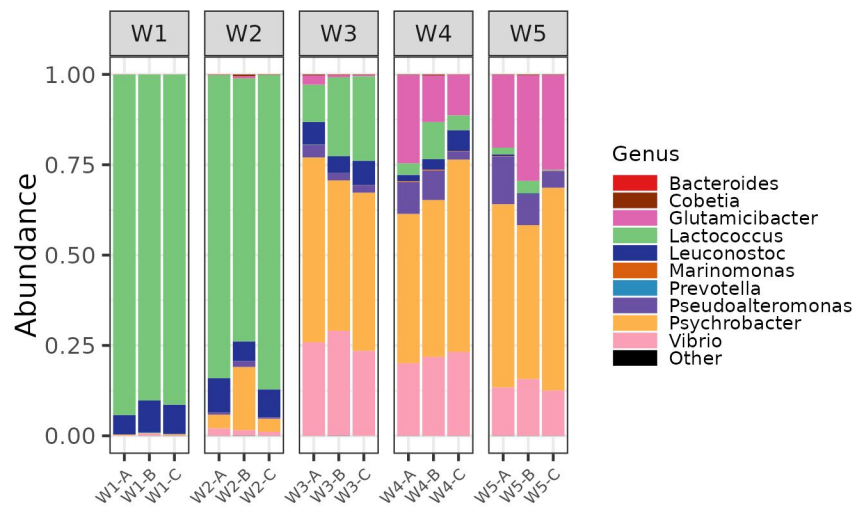
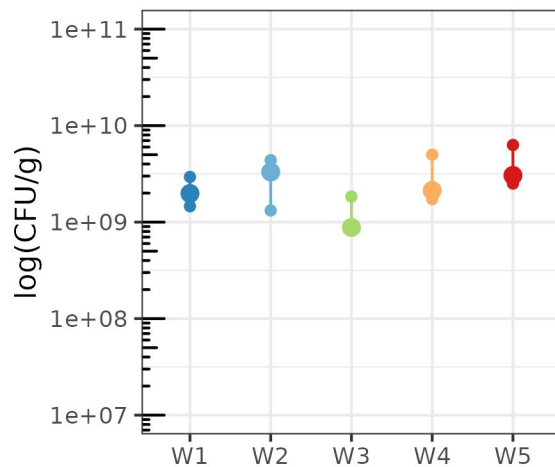
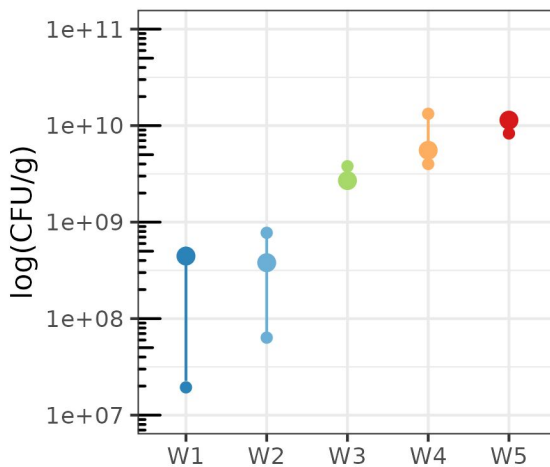
- 565 48. Guo J, Bolduc B, Zayed AA, Varsani A, Dominguez-Huerta G, Delmont TO, Pratama AA, Gazitúa  
566 MC, Vik D, Sullivan MB, Roux S. 2021. VirSorter2: a multi-classifier, expert-guided approach to  
567 detect diverse DNA and RNA viruses. *Microbiome* 9:37.
- 568 49. Nayfach S, Camargo AP, Schulz F, Eloie-Fadrosch E, Roux S, Kyrpides NC. 2021. CheckV assesses  
569 the quality and completeness of metagenome-assembled viral genomes. 5. *Nat Biotechnol*  
570 39:578–585.
- 571 50. Roux S, Camargo AP, Coutinho FH, Dabdoub SM, Dutilh BE, Nayfach S, Tritt A. 2022. iPHoP: an  
572 integrated machine-learning framework to maximize host prediction for metagenome-  
573 assembled virus genomes. preprint. *Microbiology*.
- 574 51. Vasimuddin Md, Misra S, Li H, Aluru S. 2019. Efficient Architecture-Aware Acceleration of BWA-  
575 MEM for Multicore Systems, p. 314–324. *In* 2019 IEEE International Parallel and Distributed  
576 Processing Symposium (IPDPS).
- 577 52. McMurdie PJ, Holmes S. 2013. phyloseq: an R package for reproducible interactive analysis and  
578 graphics of microbiome census data. *PLOS ONE* 8:e61217.
- 579 53. Love MI, Huber W, Anders S. 2014. Moderated estimation of fold change and dispersion for  
580 RNA-seq data with DESeq2. *Genome Biology* 15:550.
- 581 54. Escudié F, Auer L, Bernard M, Mariadassou M, Cauquil L, Vidal K, Maman S, Hernandez-Raquet  
582 G, Combes S, Pascal G. 2017. FROGS: Find, Rapidly, OTUs with Galaxy Solution. *Bioinformatics*  
583 <https://doi.org/10.1093/bioinformatics/btx791>.
- 584 55. Mahé F, Rognes T, Quince C, de Vargas C, Dunthorn M. 2014. Swarm: robust and fast clustering  
585 method for amplicon-based studies. *PeerJ* 2:e593.

- 586 56. Bokulich NA, Subramanian S, Faith JJ, Gevers D, Gordon JI, Knight R, Mills DA, Caporaso JG.  
587 2013. Quality-filtering vastly improves diversity estimates from Illumina amplicon sequencing.  
588 Nat Methods 10:57–59.
- 589 57. Yoon S-H, Ha S-M, Kwon S, Lim J, Kim Y, Seo H, Chun J. 2017. Introducing EzBioCloud: a  
590 taxonomically united database of 16S rRNA gene sequences and whole-genome assemblies. Int  
591 J Syst Evol Microbiol 67:1613–1617.

592





**A** Differentially abundant vOTUs**B** Bacterial community composition**C** Yeasts**D** Aerobic bacteria**E** Lactic acid bacteria